Dual-Band and Polarization-Flexible CRLH Substrate-Integrated Waveguide Resonant Antenna

Hanseung Lee, *Member, IEEE*, Dongyin Ren, *Student Member, IEEE*, and Jun H. Choi, *Member, IEEE*

***Abstract*—A dual-band and polarization-flexible substrate-integrated waveguide (SIW) resonant antenna based on composite right-/left-handed (CRLH) structure is presented in this letter. The proposed antenna consists of a CRLH SIW resonator and dual feeding lines. A slot and surface-mount technology capacitors on the top metallic layer of SIW resonator provide necessary reactance to realize multiresonance CRLH structure. Due to the intrinsic multiband characteristic of a CRLH structure, the proposed antenna can provide dual-band broadside radiations. Polarization flexibility is realized by two orthogonal feedlines. Utilizing the CRLH resonator instead of the conventional square resonator, such as patch antenna, allows antenna miniaturization. The electrical lengths of the sidewalls for the proposed square SIW resonant antenna are 75% (for first resonant mode) and 44% (for second resonant mode) shorter than that of the previously proposed dual-band polarization-flexible SIW antenna. To highlight the unique advantages, the dual-band circularly polarized antenna array based on the proposed antenna element is presented. Dual-band circularly polarized radiation is supported by the dual-band CRLH transmission-line-based feeding network.**

***Index Terms*—Composite right-/left-handed (CRLH), dual band, polarization, slot antennas, substrate integrated waveguide (SIW).**

I. Introduction

ANTENNAS have been key components for various communication systems [1], [2]. Single-band and single-polarized antennas may be acceptable for general consumer devices. However, advanced antennas capable of simultaneously supporting multifunctionality, higher efficiency, and compact size are highly desired for applications demanding stringent design specifications. For example, modern communication handsets have various functions and require antennas operating at multiple bands [3], [4]. Depending on specific applications, polarizations of antennas also need to be controllable [5], [6]. Under these circumstances, a dual-band and polarization-flexible (DBPF) antenna may be beneficial. A DBPF antenna can reduce overall system size and, more importantly, help to maintain stable communication link [7]–[9].

In this letter, a compact DBPF substrate integrated waveguide (SIW) resonant antenna is proposed. It provides composite right-/left-handed (CRLH) characteristic on SIW resonator to miniaturize the antenna size [10]. In comparison to the previous DBPF SIW antenna [7], the proposed antenna supports negative resonant mode, which resonates at much lower frequency than that of the conventional TE_{120} mode for the same physical dimension. In this new design, TE_{120} mode is used for the second band. Therefore, contrary to the previously proposed DBPF antenna that uses conventional TE_{120} mode for first broadside radiation, the proposed antenna behaves as an electrically miniaturized radiator. As will be discussed in Section III, such a feature can be especially beneficial when arranged in an array configuration. The proposed antenna has two orthogonal feeding lines, which provide two orthogonal linearly polarized radiations. Radiated waves with arbitrary polarization states can be generated by controlling the phase responses and magnitudes of the two orthogonally excited waves.

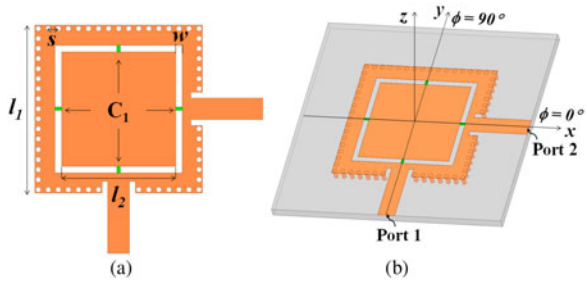

Fig. 1. (a) Top view of the proposed single antenna. (b) Perspective view and coordinators. (Parameters: $l_1 = 25$ mm, $l_2 = 17$ mm, $w = 1$ mm, $s = 1.5$ mm, and $C_1 = 3$ pF.)

II. Analysis of Antenna Element

A. Dual-Band Characteristic

Fig. 1 shows the compact DBPF SIW resonant antenna and its dimensions. The square resonator with a square slot generates broadside radiation from conventional TE_{120} resonance mode [12]. In the previously proposed antenna [7], conductor strips were added at the centers of each radiating slot etched onto the top metallic layer. The physical size of the resonator was not changed, but the effective resonator size was smaller, thereby generating second radiation at higher frequency. Since the physical resonator size corresponds with lower broadside radiation mode, the resonator length of Lee *et al.* [7] is larger than a half-wavelength at the second broadside radiation mode. However, the antenna proposed in this letter has a CRLH resonant structure in which its second broadside radiation is generated at conventional TE_{120} mode. Therefore, compared to Lee *et al.* [7] who use TE_{120} as a first radiation mode, the proposed an-

Manuscript received January 18, 2018; accepted June 18, 2018. Date of publication June 21, 2018; date of current version August 2, 2018. *(Corresponding author: Hanseung Lee.)*

H. Lee was with the University of California at Los Angeles, Los Angeles, CA 90095 USA. He is now with Skyworks Solutions, Inc., Newbury Park, CA 91320 USA (e-mail: Hanseung.lee@skyworksinc.com).

D. Ren and J. H. Choi are with the Department of Electrical Engineering, State University of New York at Buffalo, Buffalo, NY 14260 USA (e-mail: dongyinr@buffalo.edu; junhchoi@buffalo.edu).

Digital Object Identifier 10.1109/LAWP.2018.2849678

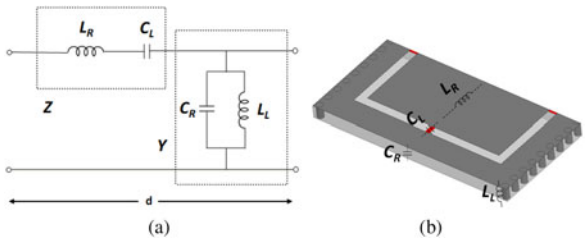

Fig. 2. (a) General circuit diagram of CRLH structure. (b) Fundamental unit cell of the proposed single antenna cavity.

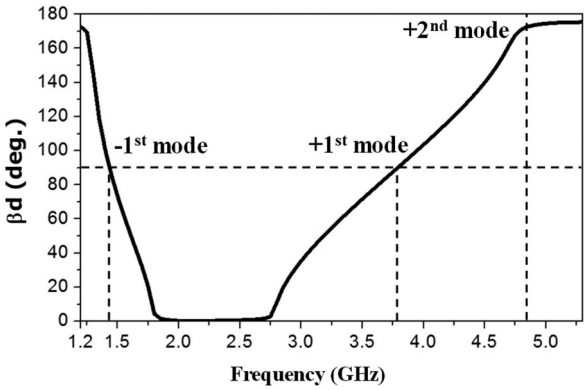

Fig. 3. Dispersion diagram of the fundamental CRLH unit cell.

tenna is electrically smaller and is better suited for array configurations. First-band broadside radiation of the proposed antenna is generated by negative resonance [11], a unique trait of a CRLH structure. General circuit diagram of a CRLH structure is shown in Fig. 2(a). Series capacitance and shunt inductance of CRLH structure enables left-handed characteristic, thereby allowing negative-mode resonances. The proposed antenna is composed with two CRLH cells. Fig. 2(b) shows fundamental CRLH unit cell of the proposed single antenna. Equivalent circuit diagram of the unit cell is the same as that of a CRLH structure. Series capacitor C_{L} is implemented by a surface-mount technology capacitor mounted across the slots on the top metallic layer of the SIW resonator. Top metallic layer and side walls provide L_{R} and L_{L}, respectively. Two metallic layers and top and bottom walls of the resonator provide shunt capacitance C_{R}. The dispersion diagram of the fundamental unit cell is shown in Fig. 3. The scattering parameters of the CRLH unit cell obtained from full-wave simulation by Ansoft HFSS are used for acquiring the dispersion diagram. For the proposed single antenna, two sidewalls opposite from the feed points are completely closed using array of vias.

The resonance frequencies for an M-stage CRLH TL can be found on the dispersion curve when the following condition is satisfied [11]:

$$\beta d = n\pi/M \tag{1}$$

where β and d are propagation constant and length of the unit cell, respectively, and n is an integer.

In the proposed antenna, the following resonant modes can be expected: $-$2nd mode ($\beta d = +180°$), $-$1st mode ($\beta d = +90°$), 0th mode ($\beta d = 0°$), $+$1st mode ($\beta d = -90°$), and $+$2nd mode ($\beta d = -180°$). For broadside radiation, the proposed antenna uses $-$1st mode and $+$2nd mode. It is found that the operating frequencies of the proposed single antenna are 1.78 GHz

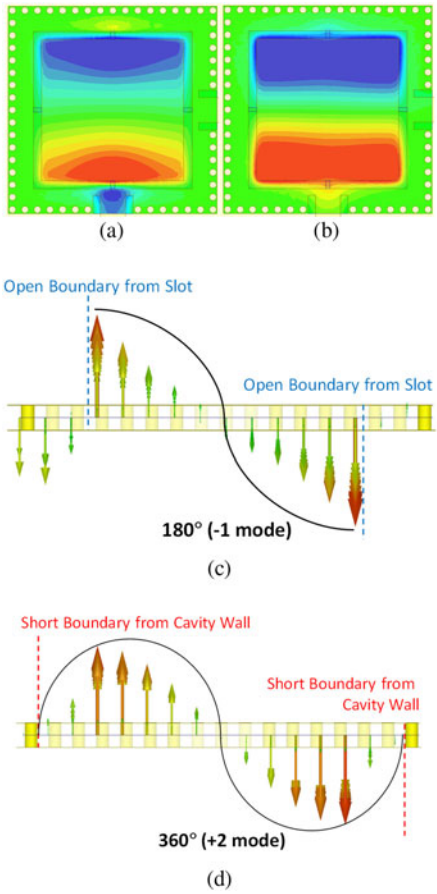

Fig. 4. Z-directed electric field distributions on xy plane: (a) first broadside radiation mode at 1.78 GHz and (b) second broadside radiation mode at 5.36 GHz. Z-directed electric field distributions on yz plane: (c) first broadside radiation mode at 1.78 GHz and (d) second broadside radiation mode at 5.36 GHz.

($-$1st mode) and 5.36 GHz ($+$2nd mode). The discrepancy between the operating frequencies and the dispersion diagram is expected because the single antenna does not have periodic boundary condition (the dispersion diagram is calculated assuming a periodic boundary condition). Also, the effect of feeding lines and matching slots is not fully considered when generating the dispersion diagram. Fig. 4(a) and (b) shows simulated electric field distributions inside SIW resonator (on xy plane) at two target frequencies. Two field distributions resemble the inside patch, but two modes encounter different boundary conditions, thereby operating at two different mode numbers. The square slot on the resonator surface provides open condition at first broadside mode. Therefore, its phase angle ($\beta d \times 2$) is 180° as shown in Fig. 4(c). In second broadside mode, conductive sidewall provides short boundaries, and conventional TE_{120} is supported. Borrowing the terminology used in a transmission-line (TL) theory, $+$2nd mode is used. Fig. 4(c) and (d) provides z-directed electric field distribution at first and second broadside modes, respectively. In Fig. 4(d), 360° phase response is observed. The first resonance is mainly controlled by C_{L} [10], and designers can control the second resonance mode by adjusting cavity and slot size [7].

B. Antenna Element Experimental Verification

Fig. 5(a) shows a photograph of the fabricated single antenna. The antenna is fabricated using RO4003C substrate ($\varepsilon_{\mathrm{r}} = 3.55$,

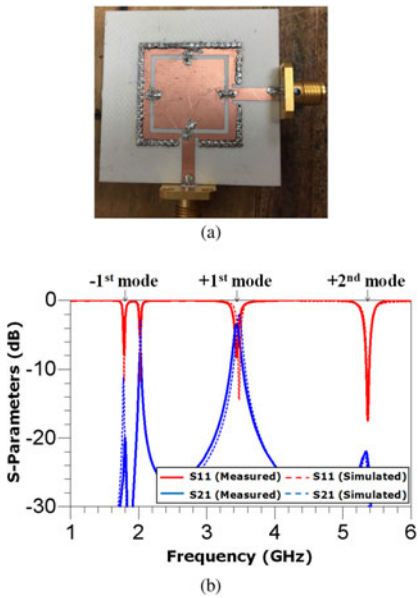

Fig. 5. (a) Photograph of the proposed single antenna. (b) *S*-parameters of the proposed single antenna.

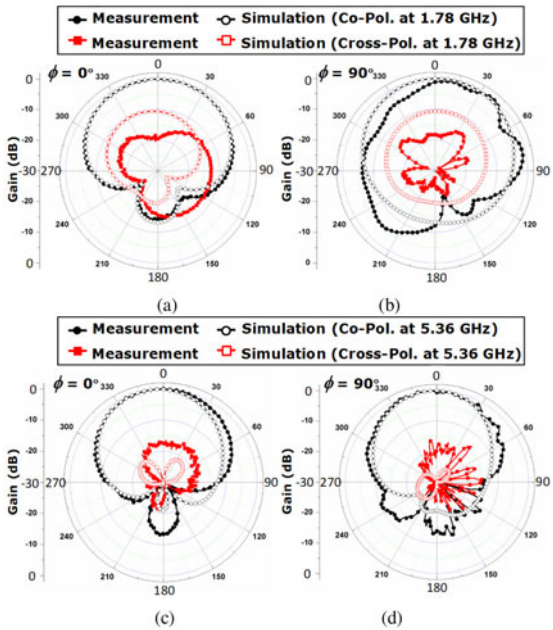

Fig. 6. Normalized gain patterns of the single antenna. The first broadside radiation modes at (a) *xz* plane and (b) *yz* plane. Normalized gain patterns of the second broadside radiation mode at (c) *xz* plane and (d) *yz* plane.

$h = 1.524$ mm). Sidewalls of SIW resonator are realized by inserting arrays of conductive vias between top and bottom metallic layers. The antenna uses Murata 0402 size capacitors. The simulated and measured *S*-parameters of the proposed antenna show a good agreement [see Fig. 5(b)]. In the first operating mode (at 1.78 GHz), the measured return loss (S_{11}) is lower than -12 dB. The measured isolation between the two ports (S_{21}) is greater than 20 dB. The second broadside radiation mode operates at 5.36 GHz. At the second operating frequency, the measured S_{11} is smaller than -18 dB, and the measured S_{21} is smaller than -22 dB. Overall, the measured *S*-parameters show a good agreement with the simulated results. Fig. 6 shows

TABLE I
COMPARISONS WITH RELEVANT WORKS

	CF (GHz)		Size (λ_g^2)		FBW (%)		Pol. Control
	f_1	f_2	f_1	f_2	f_1	f_2	
[8]	2.4	5.2	3.2	15.6	22.9	18.6	Full Control
[9]	2.4	5.8	1.4	8.2	3.6	4.2	Fixed States
[7]	13.4	17.9	1.3	2.3	1.1	2.0	Full Control
This work	1.8	5.4	0.1	0.7	0.5	0.7	Full Control

the normalized far-field radiation patterns when only Port 1 is excited (*y*-directed linear polarization). The proposed antenna shows broadside radiation patterns at both operating frequencies. Also, higher directivity can be observed for radiation at 5.36 GHz as the antenna behaves as an effectively larger radiator than when excited with 1.78 GHz waves. The measured cross-polarization levels at both frequencies are around 10 dB less than the copolarization levels on the boresight. Table I shows the comparisons with other published dual-band antennas with polarization control capability. The antenna introduced in [8] is able to fully control the polarization states. However, the antenna is electrically large and bulky. Active polarization control antenna introduced in [9] uses p-i-n diodes to switch polarization states. Compared to [8], however, it has limited polarization control capability. Lee e*t al.* [7] provide full-polarization control at relatively smaller size than [8] and [9]. The antenna proposed in this letter equipped with full-polarization control capability is more compact than all other previously realized dual-band polarization-flexible resonant antennas, as shown in Table I.

III. ARRAY ANTENNA AND EXPERIMENTAL VERIFICATION

Since the proposed antenna has compact size (electrically smaller than $\lambda_0/2$ at both operating frequencies, where λ_0 is the free-space wavelength), the proposed antenna is well suited for array configuration. To verify this advantage, a 2×2 antenna array system supporting dual-band circularly polarized radiations is designed. The proposed dual-band circularly polarized array antenna consists of the dual-band CRLH feeding network and four compact-size DBPF single antennas. To generate dual-band circularly polarized radiation, eight feeding lines connected with 2×2 DBPF antenna array are simultaneously excited with specific phase conditions at dual operating frequencies. The required phase conditions and the conceptual diagram of the dual-band feeding network are shown in Fig. 7. To satisfy these conditions, the dual-band feeding network is designed with TLs and Wilkinson power dividers. The dual-band feeding network uses both conventional TLs and CRLH TLs. CRLH TL1 shows 180° phase differences with conventional TL1 at both operating frequencies. Phase difference between CRLH TL2 and conventional TL2 (θ_0–θ_1) is $-90°$ at 1.78 GHz and $+90°$ at 5.36 GHz.

Fig. 8 shows the picture of the proposed 2×2 dual-band circular-polarization array antenna. The proposed single DBPF antenna can also be excited using vertically launched coaxial feed instead of microstrip line feeding if needed. Therefore, if desired, it is also capable of scaling to larger array dimensions.

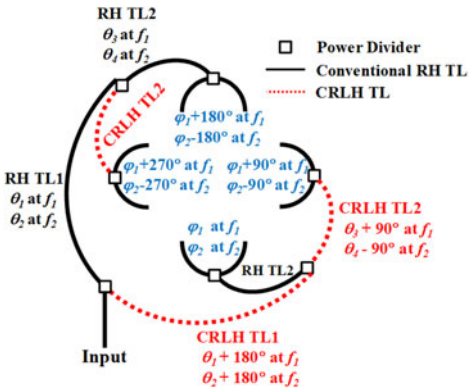

Fig. 7. Operating diagram of the dual-band feeding network for circularly polarized radiations.

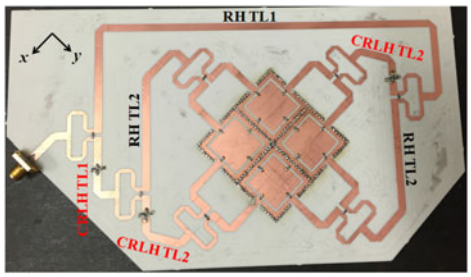

Fig. 8. Photograph of the proposed dual-band circular polarization array antenna.

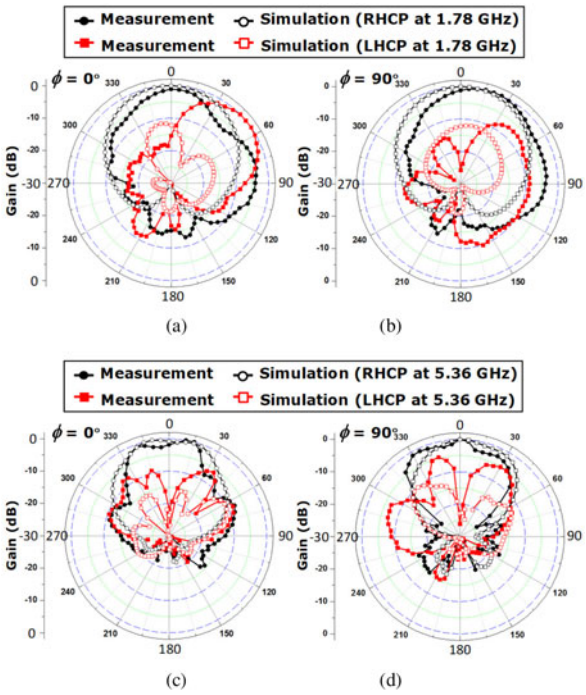

Fig. 9. Normalized gain patterns of the array antenna. The first broadside radiation mode at (a) *xz* plane and (b) *yz* plane. Normalized gain patterns of the second broadside radiation mode at (c) *xz* plane and (d) *yz* plane.

The normalized far-field patterns of the proposed array antenna are presented in Fig. 9. It is worth noting that the proposed array antenna radiates different polarization states at two operating frequencies. The antenna radiates right-hand circular polarization beam at first resonant frequency (1.78 GHz). However, it provides left-hand circular polarization radiation at second target frequency (5.36 GHz). As expected, since the antenna behaves as an electrically smaller aperture at lower frequency band, the antenna beamwidth at 1.78 GHz is wider than that at 5.36 GHz. The measured cross-polarization levels at both frequencies are less than 15 dB compared with the copolarization levels on the boresight. Discrepancies between simulated and measured results are due to fabrication and measurement errors.

IV. Conclusion

In this letter, the compact dual-band and polarization-flexible antenna is proposed. A CRLH structure is realized by adding series capacitances on an SIW resonator. The proposed antenna element supports the first broadside radiation through negative resonance, and the second broadside radiation by the conventional TE_{120} mode of the square resonator. Although the antenna provides relatively narrower bandwidth, it provides several unique advantages that may serve useful for complex wireless systems that require multifunctionalities. Since the antenna size is smaller than $\lambda_0/2$ at both operating frequencies, the proposed antenna performs well in an array configuration enabling directivity improvement and beam steering. In addition, the proposed antenna is equipped with orthogonal dual feeding lines that provide polarization-agile characteristic at both operating bands.

References

[1] C. Balanis, *Antenna Theory: Analysis and Design*. New York, NY, USA: Wiley, 2005.
[2] W. L. Stuntzman and G. A. Thiele, *Antenna Theory and Design*. New York, NY, USA: Wiley, 2012.
[3] S. Chen, D. Dong, Z. Liao, Q. Cai, and G. Liu, "Compact wideband and dual-band antenna for TD-LTE and WLAN applications," *Electron. Lett.*, vol. 50, pp. 1111–1112, Jul. 2014.
[4] Z. Wu, L. Li, X. Chen, and K. Li, "Dual-band antenna integrating with rectangular mushroom-like superstrate for WLAN applications," *IEEE Antennas Wireless Propag. Lett.*, vol. 15, pp. 1269–1272, 2016.
[5] S. Gao, A. Sambell, and S. S. Zhong, "Polarization-agile antennas," *IEEE Antennas Propag. Mag.*, vol. 48, no. 3, pp. 28–37, Jun. 2006.
[6] Y. Sung, T. Jang, and Y. Kim, "A reconfigurable microstrip antenna for switchable polarization," *IEEE Microw. Wireless Compon. Lett.*, vol. 14, no. 11, pp. 534–536, Nov. 2004.
[7] H. Lee, Y. Sung, C. M. Wu, and T. Itoh, "Dual-band and polarization-flexible cavity antenna based on substrate integrated waveguide" *IEEE Antennas Wireless Propag. Lett.*, vol. 15, pp. 488–491, 2016.
[8] J. M. Steyn, J. Joubert, and J. W. Odendaal, "A polarization diverse antenna for dual-band WLAN applications" in *Proc. Eur. Microw. Conf.*, 2009, pp. 540–543.
[9] P. Y. Qin, Y. J. Guo, and C. Ding, "A dual-band polarization reconfigurable antenna for WLAN systems," *IEEE Trans. Antennas Propag.*, vol. 61, no. 11, pp. 5706–5713, Nov. 2013.
[10] C. Caloz and T. Itoh, *Electromagnetic Metamaterials: Transmission Line Theory and Microwave Applications*. Hoboken, NJ, USA: Wiley-IEEE Press, 2005.
[11] Y. Dong and T. Itoh, "Miniaturized substrate integrated waveguide slot antennas based on negative order resonance," *IEEE Trans. Antennas Propag.*, vol. 58, no. 12, pp. 3856–3864, Dec. 2010.
[12] C. M. Wu and T. Itoh, "An X-band dual-mode antenna using substrate integrated waveguide cavity for simultaneous satellite and terrestrial links," in *Proc. Asia-Pac. Microw. Conf.*, Dec. 2014, pp. 726–728.